Low-Energy Exciton Level Structure and Dynamics in LightHarvesting Complex II Trimers from the Chl a/b Antenna Complex of Photosystem II

ARTICLE *in* THE JOURNAL OF PHYSICAL CHEMISTRY · APRIL 1994

Impact Factor: 2.78 · DOI: 10.1021/j100068a040

Low-Energy Exciton Level Structure and Dynamics in Light Harvesting Complex II Trimers from the Chl *a*/*b* Antenna Complex of Photosystem II

N. R. S. Reddy,† H. van Amerongen,‡ S. L. S. Kwa,‡ R. van Grondelle,‡ and G. J. Small*,†

Ames Laboratory–USDOE and Department of Chemistry, Iowa State University, Ames, Iowa 50011, and Department of Physics and Astronomy, Free University, Amsterdam, The Netherlands

Received: November 5, 1993; In Final Form: February 15, 1994®

Nonphotochemical hole-burned spectra obtained as a function of burn wavelength at 4.2 K are reported for the isolated LHC II peripheral antenna complex of photosystem II. The lowest-energy state of the trimer complex is shown to lie at 680 nm, 4 nm below the most intense Chl *a* band at 676 nm. The linear electron–phonon coupling for the 680-nm state is characterized and used to predict that its fluorescence origin should lie at 681 nm, precisely coincident with the observed origin at 4.2 K. The 680-nm band carries the equivalent absorption strength of about one chlorophyll *a* molecule per C_3 trimer complex, which contains about 27 chlorophyll *a* molecules. The 680-nm absorption band possesses an inhomogeneous width of $\sim$120 cm^{-1}, and its zero-phonon line distribution function is largely uncorrelated with those of the higher-energy states. Zero-phonon hole widths are used to determine that the fluorescent 680-nm state dephases in 10 ps at 4.2 K. An interpretation of this dephasing is given in terms of the trimer of subunits structure. Based on the satellite hole structure observed upon hole burning into the 680-nm state, two new states at 674 and 678 nm are identified. The possibility that these three states are excitonically correlated is considered. The observed trend in the zero-phonon hole burning efficiency as a function of burn frequency is qualitatively consistent with the states at energies higher than 680 nm having ultrashort lifetimes at 4.2 K.

I. Introduction

Optical excitation energy transfer in photosynthetic antenna is a subject of longstanding interest and very considerable difficulty.[1-6] The antenna is often comprised of several protein–chlorophyll (Chl) complexes whose organization around the reaction center (RC) serves to efficiently deliver the excitation to the special pair (primary electron donor) of the RC.[7-11] Understandably, much emphasis has been placed on the investigation of the individual, isolated complexes of antenna given that the characterization and determination of their excited-state (Q_y) electronic structure and energy cascading/equilibration dynamics are extremely relevant to the problem of the transport dynamics of the entire photosynthetic unit. However, the just stated problem for the individual complex is also challenging.

There are several reasons for this. A protein complex generally possesses a structural subunit that contains several Chl molecules bound to polypeptides.[7-9] The unit cell of the complex can be comprised of several (often three) symmetry-equivalent subunits. When center-to-center distances between Chl molecules are sufficiently short ($\lesssim$15 Å), excitonic interactions ($\geq$50 cm^{-1}) play a critical role in determining the energies and pigment compositions of the photocatalytic $Q_y(S_1)$ Chl states as well as their linear and circular dichroism spectra.[12] When the energy spacings between the exciton levels of the unit cell are greater than their energy uncertainties from bath-induced pure dephasing, application of conventional Förster theory to energy cascading (relaxation) within the exciton level manifold is inappropriate.[13,14] Adding to the complexity is the inherent glasslike structural heterogeneity of the protein which imparts significant inhomogeneous broadening to the Q_y origin absorption bands ($\sim$100 cm^{-1}) as well as distributions of values for the electronic energy gaps involved in cascading. Understanding such distributions, along with the electron- or exciton–protein phonon coupling, is important to the interpretation of the temperature dependence and dispersive kinetics of energy and electron transfer.[15-18]

Despite the complexity, considerable progress has been made in recent years on several protein–Chl complexes. At this point we mention only the Fenna–Matthews–Olson (FMO) bacteriochlorophyll *a* complex of *Prosthecochloris aestuarii* whose unit cell structure has been determined and is comprised of a C_3 trimer of subunits, each of which contains seven symmetry-inequivalent BChl *a* molecules.[19,20] The application of nonphotochemical hole burning (NPHB)[13,21] and polarized triplet–singlet difference spectroscopy[22] led to new insights on the exciton level structure of the trimer which were pivotal for much improved calculations of the absorption and circular dichroism spectra.[12,23] The hole-burning results revealed for the first time that downward energy cascading from the higher exciton levels (induced by exciton–phonon scattering[13]) is ultrafast, $\sim$100 fs, in a system where the exciton level manifold spans $\sim$500 cm^{-1}. The results also led to determinations of the inhomogeneous broadenings and linear electron–phonon coupling strengths of the Q_y transitions. For detailed discussions of the application of hole-burning spectroscopies to photosynthetic protein complexes, several review articles are available.[6,24,25]

We report here on the first NPHB study of the major Chl *a*/*b* LHC II complex associated with photosystem II of green plants and green algae. The recently reported three-dimensional structure of this complex at 6-Å resolution[26] has stimulated several new frequency[27-29] and time domain[30,31] spectroscopic studies. Important earlier works are discussed in these references. The structure reported by Kühlbrandt and co-workers[26] was determined with crystals formed from isolated, trimeric complexes. Trimeric complexes were studied in refs 27 and 28 and were used in the present work. The structure inferred from the electron diffraction density map[26] has each subunit ("monomer") of the trimer binding 15 Chls with all porphyrin rings oriented at small angles with the normal to the membrane plane (average angle is about 10°). The most recent determination for the Chl *a*/Chl *b* ratio of the trimeric complex is $\sim$1.5.[27] The Chl molecules are arranged in two layers near the upper and lower surfaces of the thylakoid membrane (eight in one and seven in the other). The C_3 axis is close to parallel with the normal to the membrane plane. The resolution of the map is not sufficient to distinguish

† Iowa State University.
‡ Free University.
® Abstract published in *Advance ACS Abstracts*, April 1, 1994.

0022-3654/94/2098-4729$04.50/0

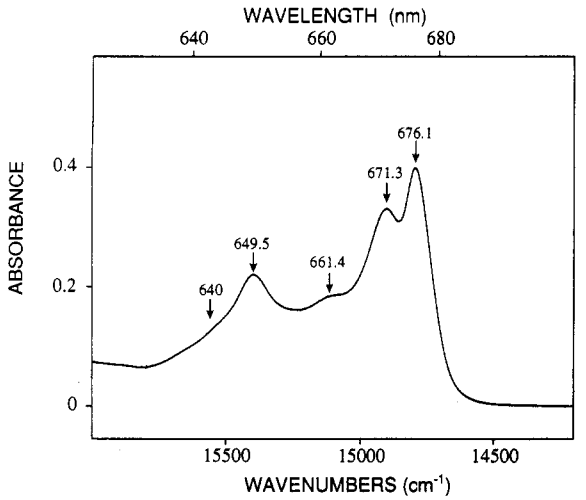

Figure 1. Low-temperature (4.2 K) absorption spectrum (Q_y region) of LHC II complex in pH 6.5 solution containing 20 mM NaCl, 0.03% (w/v) dodecylmaltoside in a glycerol:water (2:1) glass forming solution. Arrows identify the prominent absorption maxima at 676.1, 671.3, 661.4, and 649.5 nm.

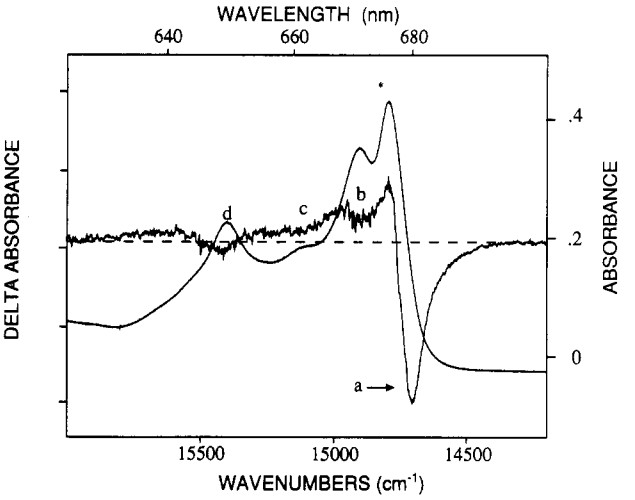

Figure 2. Hole-burned spectrum (resolution = 4 cm^{-1}) of LHC II complex obtained (at 4.2 K) with a burn wavelength of 646.8 nm (15 460 cm^{-1}). Hole was burnt for 40 min with a burn laser intensity of 100 mW/cm^2. Absorption spectrum of the sample used is shown for convenience.

between Chl *a* and Chl *b* molecules and for a determination of the Q_y transition dipole directions. In addition, it is possible that[26] the determination of 15 Chl per subunit is too high by one or two Chl. Convincing arguments for the above trimeric complex having the structure of the native conformation of LHC II are given in refs 27 and 28.

The structure obtained by Kühlbrandt et al.[26] also led to quite accurate estimates of the center-to-center distances between Chls. Nearest-neighbor distances in each of the two levels of Chls are in the range 9–14 Å. The shortest distances between Chls belonging to different levels is 13–14 Å. Thus, one could reasonably expect strong excitonic interactions in the isolated trimeric complex. This led Hemelrijk et al.[27] and Kwa et al.[28] to recently study the low-temperature (77 and/or 4.2 K) absorption, circular dichroism, and linear dichroism spectra of the trimeric complex. Their results indicate the existence of significant and complex excitonic interactions. These works also determined that the fluorescence origin at 4.2 K is shifted 5 nm to the red of the most intense, lowest-energy Q_y absorption band at 676 nm. A number of questions were raised including whether there might be a state(s) lying lower in energy than 676 nm at 4.2 K and the extent of the inhomogeneous broadening of the spectral features in the vicinity of 676 nm.[28]

These questions as well as the extent to which NPHB can shed additional light on exciton level structure and relaxation dynamics at low temperatures are addressed here.

II. Experimental Section

The trimeric LHC Section II complex was prepared and purified according to the procedure of Hemelrijk et al.[27] in which the mild detergent *n*-dodecyl-β,D-maltoside was used for solubilization during the isolation procedure. For the low-temperature spectroscopic measurements, the glass-forming solvent was buffered (Bis-Tris/NaCl) glycerol with 0.03% (w/v) dodecylmaltoside. The 4.2 K absorption spectrum of the Q_y region (Figure 1) is identical to that reported by Kwa et al.[28] Recent studies of aggregation effects have established that this absorption spectrum is characteristic of isolated trimers [van Amerongen, H., unpublished results]. Samples of the LHC II complex kindly provided to us by R. Picorel and M. Seibert yielded absorption spectra similar to that shown in Figure 1 with the major differences being lower resolution (larger inhomogeneous broadening), slight (~1.4 nm) red-shifting of the features at 676.0 and 649.5 nm, and enhanced intensity around 662.3 nm. However, the hole-burning results obtained (not shown) are similar to those presented below.

The apparatus used for the absorption and hole-burning measurements was the same as described elsewhere.[32] Briefly, hole burning employed a Coherent CR699-21 laser (line width ~ 0.05 cm^{-1}) pumped by a 6-W Coherent Innova argon ion laser. Hole and absorption spectra were read with a Bruker HR Fourier transform spectrometer. All reported results were obtained for a sample temperature of 4.2 K (convection cooling liquid helium cryostat). Hole-burning conditions and read resolution are given in the figure captions.

III. Results

The 4.2 K absorption spectrum (Figure 1) exhibits four partially resolved bands at 676.1, 671.3, 661.4, and 649.5 nm plus unresolved absorption in the vicinity of 641 nm, which is too intense to be accounted for completely in terms of vibronic transitions building on the intense origin bands at 676.0 and 671.3 nm. Thus, only five features are apparent from the over 40 Chl *a* and Chl *b* contributing molecules. (Chl *a* and Chl *b monomer* molecules absorb near 667 and 650 nm.) In what follows, we will refer to the wavelengths of the above bands as 676, 671, 661, and 650 nm.

Hole burning was performed with burn wavelengths (λ_B) between 681 and 649 nm. Zero-phonon hole (ZPH) burning efficiency was observed to decrease markedly for λ_B values lower than ~676 nm (by a factor of ≳20). Before showing the ZPH data obtained with $\lambda_B \geq 676$ nm, we show one hole-burned spectrum in Figure 2 which is quite typical of those obtained with lower λ_B values. The hole spectrum in Figure 2, obtained with $\lambda_B = 646.8$ nm, is close to saturated; that is, the holes have attained maximum depth. It consists of four broad lower-energy holes (a–d) with the last three appearing to be coincident with the absorption bands at 650, 661, and 671 nm. The most intense feature is hole a whose blue-shifted antihole is located by the asterisk. It is well established that the antihole associated with burning of $\pi\pi^*$ states in proteins, glasses, and polymers is blue-shifted with a peak intensity which is about equal to that of the hole it is associated with.[18,24,33-35] The expected intensity and location of the antihole maximum in Figure 2 are given by the asterisk. The smaller than expected intensity observed is discussed in the following section. A key observation is that hole a is located at 14 710 cm^{-1} (679.8 nm), which is 90 cm^{-1} to the red of the 676-nm absorption band. Its energy is invariant to λ_B. As discussed in the following section, hole a is due to NPHB in a

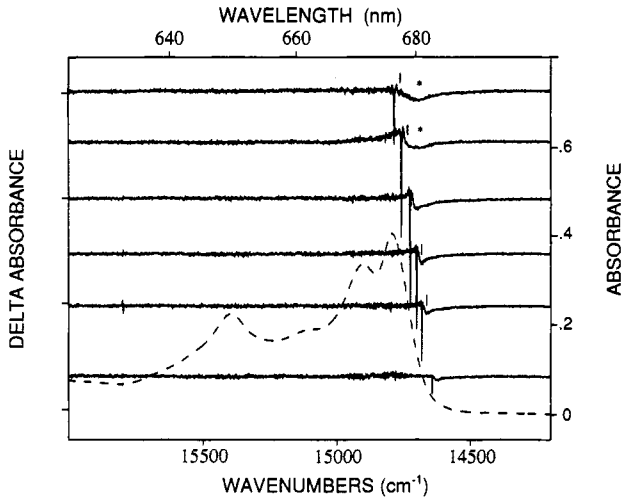

Figure 3. Hole-burned (Δ absorbance) spectra of LHC II complex obtained at various burn wavelengths (resolution = 4 cm^{-1}) in long-wavelength region of Q_y absorption. Typical burn conditions for obtaining the hole-burned spectra were 50 mW/cm^2 for 5 min. Burn wavelengths (in nm) for the various hole-burned spectra are (from the top) 676.3 (14 787 cm^{-1}), 677.5 (14 761 cm^{-1}), 679.0 (14 727 cm^{-1}), 680.1 (14 703 cm^{-1}), and 681.0 (14 684 cm^{-1}). Fractional absorbance changes for these holes (from the top) are 0.09, 0.20, 0.36, 0.38, 0.43, and 0.31, respectively.

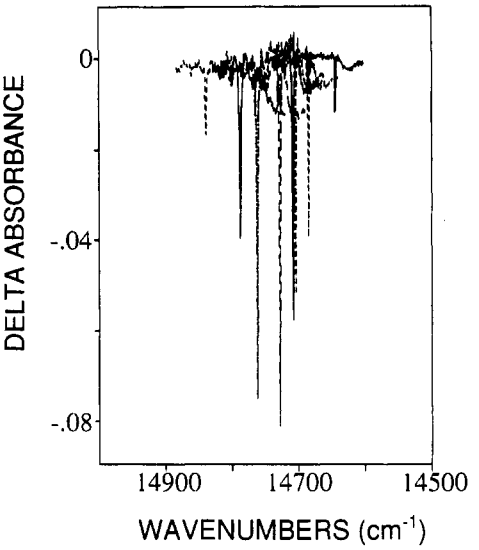

Figure 4. Constant-fluence hold-burned spectra of LHC II complex. Burn conditions and burn wavelengths used are given in the caption to Figure 3. The action spectrum can be fitted to a Gaussian profile (fwhm ~ 110 cm^{-1}).

state at 679.8 nm (referred to hereafter as the 680-nm state), which is populated from higher-energy states by energy transfer, a phenomenon that has been observed in several complexes.[18,34,37] On the basis of these works, one might anticipate[38] that the width (110 cm^{-1}) of hole a is primarily due to inhomogeneous broadening because of the absence of significant correlation between the site excitation energy distribution function of the 680-nm state and those of the higher-energy states.

To determine whether or not hole a in Figure 2 is inhomogeneously broadened, we employed ZPH-action spectroscopy which was first introduced by Reddy *et al.*[39] Here one employs constant burn fluence for different burn wavelengths in the region of the state of interest. The results for the LHC II complex are shown in Figure 3 for six of the eight burn wavelengths used. The spectra were measured with a read resolution of 4 cm^{-1}. We focus first on the relatively sharp ZPH of each spectrum which is coincident with the burn frequency. The fractional absorbance changes for the ZPH are given in the caption to Figure 3. The six ZPH of Figure 3 along with the ZPH for two other burn wavelengths are shown in Figure 4. Measurement of the ZPH intensities relative to the zero of the Δ absorbance base line of the spectra shown in Figure 3 yielded a center frequency for the ZPH action spectrum of ~14 720 cm^{-1}, which, within experimental uncertainty, is equal to the frequency of the 14 710-cm^{-1} hole (a) in Figure 2. The width of the ZPH-action spectrum is about 120 cm^{-1}, which is close to the value of 110 cm^{-1} for hole a of Figure 2. We conclude, therefore, that the 680-nm state identified from Figure 2 is responsible for the ZPH-action spectrum of Figure 4. The observation of the zero-phonon holes proves that the width of the weak absorption band of the 680-nm state is due mainly to inhomogeneous broadening.

We return now to consider other aspects of the hole spectra in Figure 3. In each of the top two spectra, one observes a broad hole located by an asterisk at 14 710 cm^{-1} with a width of about 110 cm^{-1}. Therefore, this hole corresponds to hole a of Figure 2. Also visible in the upper of these two spectra is a weaker feature (dash) which is displaced from the ZPH by 20 cm^{-1}. This is the pseudophonon sideband hole (pseudo-PSBH) commonly observed to be associated with the Chl ZPH in protein complexes.[13,18,32,38,39] As the burn frequency is tuned to the red, there is a diminution in the intensity of the broad hole at 14 710 cm^{-1} until, in the lowest two spectra, one is left with only the pseudo-PSBH. The conclusion to be reached from this behavior is clear. The broad hole at 680 nm is the result of excitation of the state(s) associated with the main absorption band at 676 nm which subsequently transfer energy to the state at 680 nm. As λ_B is tuned further to the red from 676 nm, the probability of exciting the former state(s) decreases until it approaches zero. The quite symmetric ZPH-action spectrum of Figure 4 indicates that it is the 680-nm state which is responsible for the ZPH, consistent with the earlier mentioned observation that burning of ZPH becomes highly inefficient for $\lambda_B < \sim 676$ nm. The ratio of integrated intensity of the pseudo-PSBH to that of the ZPH can be used to obtain[18,40] an upper limit for the Huang–Rhys factor S associated with protein phonons of mean frequency $\omega_m \sim 20$ cm^{-1}. (It is only in the shallow burn limit that this ratio equals S.) From the lower two spectra in Figure 3, we obtained a value of 0.5 for this limit; i.e., as has been observed for all antenna protein complexes,[6] the linear electron–phonon is weak ($S < 1$). In NPHB the real-PSBH at the frequency of the ZPH + ω_m is interfered with by the positive going antihole of the pseudo-PSBH.[42] Nevertheless, under close inspection the real-PSBH could be clearly discerned in some of the spectra; see for example the second spectrum of Figure 3. From such spectra we estimated a value of 0.4 for S. In what follows we use a value of $S = 0.4$. With this value the phonon-reorganization energy for the 680-nm state, given by $S\omega_m$, is 8 cm^{-1}, about the same as that for the lowest exciton level of the FMO complex. As discussed in the following section, this determination is important for the assignment of the state responsible for the aforementioned fluoresence origin band at 681 nm (4.2 K).

To conclude this section, we note that the spectra of Figure 3 show that hole burning of the 680-nm state elicits no strong response from the higher-energy absorption bands.

IV. Discussion

Taking the number of Chls in the trimeric LHC II complex to be 45, there are 15 doubly degenerate and 15 nondegenerate exciton levels that can contribute to the absorption spectrum of Figure 1. The former and latter levels would be polarized perpendicular and parallel to the C_3 axis (provided structural heterogeneity between the subunits of the trimer is not too severe[43]). A similar situation exists for the trimeric FMO complex of *P. aestuarii*[13] which was briefly discussed in the Introduction. Since a high-resolution X-ray structure of the FMO complex is known, exciton-type calculations are particularly informative.[12,23] In addition to the fact that the oscillator strengths of the exciton

levels can be markedly different, state (exciton level) compositions (in terms of contributing Chls) can be also when the Chls of the subunit are symmetry-inequivalent, as is the case for the FMO complex and the LHC II complex (although some local diad symmetry exists in the latter[26]). Thus, it would be imprudent to assume that a single state is responsible for each of the partially resolved absorption bands in Figure 1. Indeed, the low-temperature linear dichroism (LD) and circular dichroism (CD) spectra reveal the existence of nine states in the Q_y region.[27]

A. Assignment of the Lowest-Energy State Responsible for Fluorescence. In order to identify the state responsible for fluorescence, we obtained a 4.2 K fluorescence spectrum (not shown) of the same sample that was used in the hole-burning experiments. The fluorescence spectrum consists of a single band peaking at 680.6 nm with a full width at half-maximum of 7 nm. This spectrum, although slightly broader, is very similar to that reported by Kwa et al.,[28] who suggested that the state(s) responsible for the fluorescence might be associated with the most intense absorption band at 676 nm (Figure 1). However, Kwa et al.[28] noted that such an assignment is tentative given the possible existence of inhomogeneous broadening as well as other complicating factors. If states absorbing at ~676 nm are responsible for the fluorescence origin, then the Stokes shift is 5 nm or 110 cm^{-1} at 4.2 K. The Stokes shift is given by $2S\omega_m$ so that for our measured value of ω_m (mean phonon frequency), 20 cm^{-1}, the Huang–Rhys factor equal 2.5. Such a value is 40% higher than that observed for the primary electron donor states, P870* and P960*, of the RC of *Rb. sphaeroides* and *Rps. viridis*.[43,44] But these are states that are characterized by significant charge-transfer character.[45,46] Furthermore, hole-burning studies of many antenna protein complexes, including B800–B850 and B875 of *Rb. sphaeroides*,[38,39] the FMO complex of *P. aestuarii*,[13,21] the core complex of PS I,[47] and the CP47 and CP43 complexes of PS II,[48] have revealed that the electron–phonon coupling is weak ($S \lesssim 0.5$) with $\omega_m \sim 20$ cm^{-1}. Thus, an assignment of the fluorescence origin of LHC II to the 676-nm absorbing state(s) seems most implausible.

We explore, therefore, whether or not the new state at 680 nm (14 710 cm^{-1}) identified above can be assigned as the fluorescent state. For this state $S \sim 0.4$ and $\omega_m = 20$ cm^{-1} (*vide supra*), meaning that its fluorescence origin should lie at 14 694 cm^{-1}. This energy is equal, within experimental uncertainty, to that of the fluorescence origin (14 695 cm^{-1}). Furthermore, the ~140-cm^{-1} width of the fluorescence origin band is close to the value of 120 cm^{-1} for the absorption band of the 680-nm state. We conclude that the state responsible for the fluorescence at 4.2 K lies at 680 nm. That the 680-nm state is the dominant fluorescer strongly supports its assignment as the lowest-energy state of the LHC II trimer complex at 4.2 K.

It should be noted, however, that Kwa et al.,[28] on the basis of their 4.2 K linear dichroism spectra, deduced that *very* weak absorption exists between about 685 and 700 nm. They estimated that this absorption represents only about 1% of the absorption due to all Chl *a* molecules, i.e., ~0.3 Chl *a* per complex. The profile of hole a (from the 680-nm state) in Figure 2 is consistent with their findings. The lower-energy half of the hole exhibits a deviation (tails more slowly) from a Gaussian. The tailing becomes noticeable at ~684 nm. Subtraction of a Gaussian profile, which fits the upper approximately two-thirds of the inhomogeneously broadened hole of the 680-nm state, from the observed profile yielded a residual hole centered at 684 nm with a width of ~180 cm^{-1}. The integrated intensity of this residual hole relative to that of the 680-nm state is 0.25 ± 0.10. This value leads to the residual absorption constituting ~1.1 ± 0.2% of the total Chl *a* absorption, in excellent agreement with the value of Kwa et al.[28] As to the nature of this very weak absorption, one can conclude that it is not intrinsic to all LHC II complexes in the frozen sample since, if it were, it would be difficult to understand why the 4.2 K fluorescence does not originate from the Chl *a* (state) responsible for the absorption. The 684-nm absorption might be due to a small amount of damaged complex or aggregates of the trimeric complex.[49] However, the recent room temperature absorption results of Jennings et al.[50] suggest another possibility. Based on an unconstrained multi-Gaussian fit of the room temperature absorption spectrum, bands at 684 and 693 nm were identified. Their intensities correspond respectively to 14 and 1.5% of the intensity of the entire Q_y absorption system. Bands at 649, 659, 669, and 677 nm with intensities of 22, 19, 20, and 23% were also identified. These fitting results have been confirmed by Zucchelli et al.,[51] who report also on the 10 K absorption and linear dichroism spectra of the trimeric LHC II complex. Importantly, their 10 K absorption spectrum is essentially identical to that given here (Figure 1). The unconstrained multi-Gaussian fit of this spectrum showed no evidence for bands at 684 and 693 nm. Furthermore, the loss of 684-nm intensity appears to be compensated for by an increase in intensity of the ~670-nm band; see Figure 1. In addition, a weak band at 681 nm (intensity of 2.2%) was identified which is not seen from the fit to the room temperature spectrum. This band most likely corresponds to the 680-nm band identified here. Also relevant is the room temperature static fluorescence spectrum of Jennings et al.[52] which exhibits an origin band at 682.5 nm. This result together with the results of Jennings et al.[50] and Zucchelli et al.[51] establish that the aforementioned 693-nm band is not intrinsic to the LHC II complex, i.e., is not associated with the lowest-energy state of LHC II. Although an unconstrained multi-Gaussian fitting to room temperature spectra with little structure can be misleading, we cannot exclude the possibility, suggested by Zucchelli et al.,[51] that the 684-nm band is extremely temperature-sensitive. That is, the structural arrangement of the Chl *a* molecules responsible for this band might be temperature dependent. If so, the very weak absorption we observe at 684 nm might be the 4.2 K remnant of a much more intense 684-nm band at room temperature. For the bulk of the sample, cooling-induced structural rearrangement could, conceivably, lead to a redistribution of absorption intensity between the exciton levels. Detailed temperature-dependent studies would appear to be required to test this possibility.

B. Nature of the Fluorescent 680-nm State. Two approaches were used to estimate the integrated absorption intensity of the 680-nm state relative to that of the intense band at 676 nm. The first stems from the observation that the low-energy side of the 676-nm absorption band tails more slowly than a Gaussian. Under the assumption that the tailing is due to the 680-nm state with a Gaussian absorption and width of 120 cm^{-1} (*vide supra*), we determined a value for the above ratio of 0.1 ± 0.02. The second approach was based on the observation that the saturated ZPH depth close to 680 nm corresponds to a fractional absorbance change of about 0.4. Recognizing that the maximum fractional absorbance change for the ZPH associated with the 680-nm state is $\exp(-S)$,[40] our measured value of $S \sim 0.4$ was used to determine a value of 0.20 ± 0.05 for the intensity ratio. For what follows we use the average of the two determinations. As noted in ref 27, the states absorbing in the vicinity of 650 nm are expected to be contributed to mainly by Chl *b* molecules. Those absorbing to lower energy of ~665 nm are expected to be contributed to mainly by Chl *a* molecules. A somewhat arbitrary division of the absorption spectrum in Figure 1 at 662 nm into mainly Chl *a* and Chl *b* absorbing regions led to the estimate that the 680-nm state carries 4.5 ± 0.5% of the total Chl *a* absorption. Since we are dealing with a complex whose structure suggests the existence of strong Chl–Chl excitonic interactions, the use of this result to determine the actual number of Chl *a* molecules associated with the 680-nm state is questionable.[23] Nevertheless, we give this number because of its usefulness for what follows. Choosing the number of Chl *a* molecules in the trimer to be 27 (as in ref 26),

it is 1.2 Chl *a* molecules per trimer. Considering the uncertainties we use a value of one Chl *a* molecule per trimer in what follows.

The question is whether the 680-nm state is localized on one Chl *a* of a subunit of the trimer or a delocalized state of the trimer. The finding that the 680-nm state has the equivalent absorption strength of one Chl *a* molecule per trimer, and the results of Figure 3 might appear to support the first interpretation. As mentioned, the results of Figure 3 indicate that the response of the states contributing to the higher-energy absorption bands is weak. By way of contrast, quite intense high-energy satellite hole structure was observed upon burning ZPH in the lowest-energy exciton level of the FMO trimer complex[13,21] as well as the lowest exciton level associated with B850 and B875 of the antenna complex of *Rb. sphaeroides*.[38,39] All three of these lowest exciton levels make a weak contribution to the overall Q_y absorption spectrum. Most recently,[32,53] the upper dimer component of the special pair of *Rps. viridis* was definitively assigned on the basis of the response of the Q_y absorption spectrum to selective nonphotochemical hole burning of the lower dimer component (P960). However, the hole spectra of Figure 3 were obtained with relatively low burn fluences, and for this reason, the actual response of the higher-energy bands to hole burning in the 680-nm state is better assessed from hole spectra of the type shown in Figure 2. Even though the hole spectrum in Figure 2 was obtained with λ_B = 647 nm, the hole burning occurs in the 680-nm state because of rapid energy relaxation to it from the higher-energy states. Rapid relaxation is also responsible for our inability to burn ZPH at λ_B values located in the higher-energy bands under the burn fluence condition used to obtain the hole spectra in Figure 3. It was found that the ZPH burning efficiencies for the absorption bands to higher energy of 680 nm are about 2 orders of magnitude lower than that for the 680-nm band. The highest-energy satellite hole (d) in Figure 2 occurs near the maximum of the Chl *b* absorption band at 650 nm. However, much of the intensity of this hole can be accounted for in terms of a ~720-cm^{-1} vibronic (excited-state vibration) with a Franck–Condon factor of 0.05[18] which builds on the origin hole at 680 nm. The b anc c satellite holes cannot be assigned as vibronic features. Therefore, they might be responses from states which are excitonically correlated with the 680-nm state. Correlation means that states share common Chl molecules. Given the C_3 symmetry of the LHC II complex, the equivalent absorption strength of only one Chl per trimer for the 680-nm state, and that the b and c satellite holes are quite weak, one is led to consider the possibility that the 680-nm state is mainly associated with three symmetry-equivalent Chl molecules, one in each subunit. Ignoring structural heterogeneity between the three subunits, this situation would give rise to one nondegenerate state polarized parallel to C_3 had one doubly degenerate state polarized in the plane perpendicular to C_3. (For severe enough structural heterogeneity, these perfect polarizations would not be observed and the degenerate state could be split.[42]) The point is that the parallel and perpendicular to C_3 states should have the absorption strength of about three Chl molecules. Since we determined that the 680-nm state has the strength of one Chl, the question arises as to whether the satellite holes have, in combination, the absorption strength of about two Chl molecules. The hole spectrum of Figure 2 is not well suited for addressing this question due to the fact that the antihole of the 680-nm hole lies very close to the maximum of the 676-nm absorption band. A more suitable hole-burned spectrum is shown in Figure 5. This spectrum is for an LHC II sample from a different batch which, however, was prepared according to the same procedure used for the samples whose spectra are shown in Figures 1–4. The absorption maximum near 14 800 cm^{-1} (676 nm) is unshifted from the corresponding band in Figure 1. However, the maximum of the 680-nm hole is shifted 15 cm^{-1} to the red of the corresponding hole in Figure 2. A comparable shift and hole spectrum were

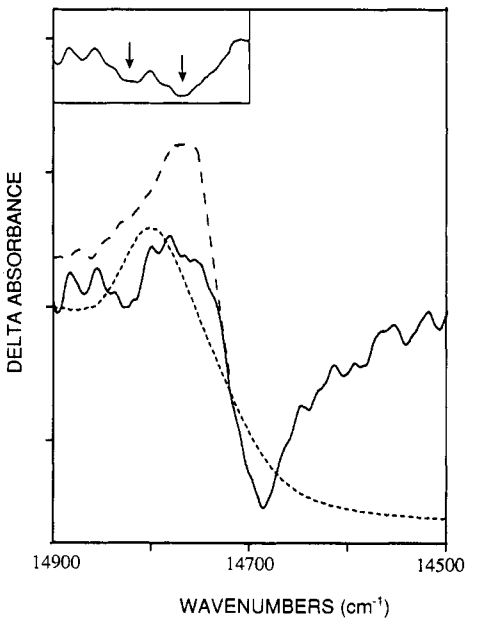

Figure 5. Hole-burned spectrum of LHC II complex. Burn conditions are λ_B = 661.2 nm (15 123 cm^{-1}), burn fluence = 100 mW/cm^2 for 40 min, and read resolution = 4 cm^{-1}. Inset shows additional holes at 14 830 and 14 755 cm^{-1} in the hole–antihole difference spectrum.

observed for the other LHC II sample mentioned in section II. The shifting leads to a comparable red shift for the antihole of the 680-nm hole. The dashed curve in Figure 5 is an approximation of the antihole that would be observed in the absence of interferences. It was obtained by inversion of the 680-nm hole through the higher-energy zero crossing point of the hole. Such an antihole has been observed for several antenna protein complexes,[18,21,38,39] although with an antihole peak intensity that is typically about 20% lower than predicted by the above procedure (a consequence of the antihole being broader than the hole). To account for the differences in the antihole intensity and width (compared with the hole on which it builds), the antihole profile obtained by hole profile inversion is reduced in intensity by 20% and broadened by the same amount. Subtraction of the hole-burned spectrum from this antihole profile (inset in Figure 5) reveals two holes (arrows) at about 14 830 cm^{-1} (674.3 nm) and 14 755 cm^{-1} (677.7 nm) to the red and blue of the 676-nm absorption band. There is a relatively weak hole feature near 670 nm (not shown but seen in Figure 2), and the tailing of the antihole (Δ absorbance > 0) out to ~650 nm seen in Figure 2 was also observed. We determined that the combined integrated intensity of the two satellite holes at 674 and 678 nm is about 80% the intensity of the 680-nm hole. The intensity of the 670-nm hole is about 20% that of the 680-nm hole. However, the complexity of the situation should be underscored. For example, the antihole of the 678-nm hole interferes with the 674-nm hole whose antihole interferes with the 670-nm hole. The end result is severe tailing of the overall antihole out to ~650 nm. This leaves open the possibility that the combined intensity of the satellite holes might be equivalent to the absorption intensity of more than one Chl *a* molecules per trimer. The results are consistent with the 680-nm state being excitonically correlated with higher-energy states. However, the results are not consistent with the 680-nm state being an exciton component of a trimer of a symmetry-equivalent Chl *a* molecule belonging to each subunit since more than one satellite hole is observed. Unfortunately, the low resolution of the LHC II electron diffraction map[26] precludes excitonic calculating that might aid in the interpretation of the hole-burning results. We hasten to add that the intepretation which would have the 680-nm state being due to a single Chl *a* molecule of the trimer would demand a complete breakdown of C_3 symmetry.

C. Dynamics. We begin with a discussion of the ZPH widths associated with the inhomogeneously broadened absorption band of the 680-nm state. A high-resolution study of the dependence of the hole width on the burn frequency (of the type reported in refs 21 and 38 on other complexes) was not undertaken. Rather, high-resolution scans were restricted to near center of the 680-nm absorption band (read resolution of 0.5 cm^{-1}). For shallow holes (<10% absorbance change), a width of 2.1 cm^{-1} was obtained at 4.2 K. The same width was obtained for a sample from a different preparation; cf. section II. This width corresponds to a total dephasing time of $T_2 = 10$ ps. As discussed in ref 38, this time is far too short to be ascribed to pure dephasing/spectral diffusion due to the glasslike low-energy excitations of the protein. Fast dephasing has been observed for the lowest exciton level in several other complexes; the lowest exciton level for B850 in the isolated B800–B850 complex of *R. sphaeroides*, of B875 in chromatophores or the isolated complex of *Rb. sphaeroides*, and of the FMO complex of *P. aestuarii*. The T_2 (4.2 K) values for these systems are 6.6,[38] 6.6,[38] and 40[21] ps. We believe that these dephasing times are most probably a consequence of the complexes being trimers of subunits which are not energetically equivalent due to structural heterogeneity of the protein. Under certain conditions the dephasing could be a measure of the time for excitation transfer between subunits of the trimer. For adequate theoretical analysis, knowledge of the relative magnitudes of the relevant excitonic interactions between Chl molecules belonging to different subunits and the diagonal energy (excitation) disorder between subunits is required.

The ZPH action spectrum in Figure 4 and the action spectrum obtained for a different LHC II preparation (not shown, see section II) are quite highly symmetric with the latter spectrum displaced to the red of the former by 30 cm^{-1}. There is *no* apparent contribution to the action spectra from states that lie to higher energy of the 680-nm state. As mentioned, the ZPH burning efficiencies for bands higher in energy than 680 nm are about 2 orders of magnitude lower than for the 680-nm state. This indicates that the T_1 (population decay) times for the higher-energy states are considerably shorter than that of the fluorescent 680-nm state. This follows because the growth of the ZPH is governed by an integrand that contains the term $\exp(-P\sigma\phi\tau)$ where P is the burning photon flux, σ is the peak absorption cross section of the ZPL, τ is the burn time, and ϕ is the quantum yield for NPHB, $\sim k_{NPHB}/(T_1^{-1})$.[54] The absorption cross section is proportional to the total dephasing time T_2 with $T_2^{-1} = (T)^{-1} + (T_2^*)^{-1}$ and T_2^* the pure dephasing time. For an illustrative calculation we consider that the T_2 value of 10 ps measured for the 680-nm state corresponds to a T_2^* process associated with "isoenergetic" scattering/trapping of a subunit excitation with the other two subunits of the trimer and that $T_2^* \sim 10$ ps for all states of LHC II. Then for two states with $T_1 = 100$ ps and 1 ps the hole burning efficiency of the $T_1 = 1$ ps state would be about 2 orders of magnitude lower (assuming k_{NPHB} is the same for both states). It must be emphasized, however, that although ZPH were observed with λ_B in the region between about 670 and 660 nm, much more detailed studies are required to exclude the possibility that they are due to Chl molecules which are not fully functional. In this regard we note that we were not able to burn a discernible ZPH into the Chl *b* band at 650 nm. This seems consistent with the recent determination by Du et al.[55] that Chl *b* → Chl *a* energy transfer occurs in ~250 fs. This ultrafast relaxation would correspond to a ZPH width of 40 cm^{-1}. Earlier it was noted that the broad hole at ~650 nm in Figure 2 can be ascribed mainly to a ~720-cm^{-1} vibronic which builds on the origin hole at 680 nm. Thus, this vibronic satellite hole would serve to obscure a ZPH with a width as large as 40 cm^{-1}. Returning to the apparent absence of ZPH for the 678-nm state, we note that if it is excitonically correlated with the 680-nm state, as we have suggested, its lifetime could be expected to be considerably shorter than 1 ps in the low-temperature limit. The higher exciton levels of the FMO complex of *P. aestuarii* were shown by hole burning to undergo energy cascading in ~100 fs[13] at 4.2 K. This ultrafast cascading has recently been confirmed by femtosecond time domain studies.[56] In ref 13 the mechanism for cascading was argued to be of the Davydov phonon emission type[14] (non-Förster) for which librational modes of Chl molecules are the promoters. The same physics was used to explain why the B850 and B875 absorption bands of the antenna of *Rb. sphaeroides* carry homogeneous widths of ~200 cm^{-1} at 4.2 K.[38] Supporting this type of interpretation are much earlier results for the S_1 exciton band of organic crystals, e.g., naphthalene, phenanthrene, and anthracene. They show that while the upper Davydov (dimer) component at liquid helium temperatures undergoes downward scattering via phonon emission in ~50 fs (corresponding to an uncertainty broadening of ~100 cm^{-1}), it is conceivable, given the structure of the LHC II complex, that the above mechanism may be important for relaxation of the higher-energy states as well.

Acknowledgment. Research at the Ames Laboratory was supported by the Division of Chemical Sciences, Office of Basic Energy Sciences, U.S. Department of Energy. Ames Laboratory is operated for USDOE by Iowa State University under Contract W-7405-Eng-82. Research at Free University was supported by the Dutch Foundation for Biophysics (SvB), financed by the Netherlands Organization for Scientific Research (NWO). We thank G. Fleming and W. Struve for useful discussions and R. Bassi and J. Breton for permission to discuss the results in ref 51 prior to publication.

References and Notes

(1) Geacintov, N. E.; Breton, J. In *Critical Reviews in Plant Science*; Congor, B. V., Ed.; CRC Press: Boca Raton, FL, Vol. 5, p 1 (1987).
(2) Pearlstein, R. M. In *Photosynthesis: Energy conversion by plants and bacteria*; Govindjee, Ed.; Academic Press: New York, 1982; p 293.
(3) van Grondelle, R. *Biochim. Biophys. Acta* **1985**, *811*, 147.
(4) Hunter, C. N.; van Grondelle, R.; Olsen, J. D. *Trends Biochem. Sci.* **1989**, *14*, 72.
(5) Knox, R. S. In *Encyclopedia of Plant Physiology*; Staehelin, L. A., Arntzen, C. J., Eds.; Springer-Verlag: Berlin, 1986; Vol. 19, p 286.
(6) Reddy, N. R. S.; Lyle, P. A.; Small, G. J. *Photosynth. Res.* **1992**, *311*, 167.
(7) Zuber, H. *Trends Biochem. Sci.* **1986**, *11*, 414.
(8) Zuber, H.; Brunisholz, R. N. In *Chlorophylls*; Scheer, H., Ed.; CRC Press: Boca Raton, FL, 1991; p 627 and references therein.
(9) Breton, J.; Nabedryk, E. In *The Light Reactions*; Barber, J., Ed.; Elsevier: Amsterdam, 1987; p 159.
(10) Kramer, H. J. M.; van Grondelle, R.; Hunter, C. M.; Westerhuis, W. H. J.; Amesz, J. *Biochim. Biophys. Acta* **1984**, *765*, 156.
(11) Kleinherenbrink, F. A. M.; Deinum, G.; Otte, S. C. M.; Hoff, A. J.; Amesz, J. *Biochim. Biophys. Acta* **1991**, *1099*, 175.
(12) Pearlstein, R. M. In *Chlorophylls*; Scheer, H., Ed.; CRC Press: Boca Raton, FL, 1991; p 1047.
(13) Johnson, S. G.; Small, G. J. *J. Phys. Chem.* **1991**, *95*, 471.
(14) Davydov, A. S. *Theory of Molecular Excitons*; Plenum Press: New York, 1971.
(15) Jortner, J. *Biochim. Biophys. Acta* **1980**, *594*, 193.
(16) Lyle, P. A.; Struve, W. S. *J. Phys. Chem.* **1991**, *95*, 4152.
(17) Small, G. J.; Hayes, J. M.; Silbey, R. *J. Phys. Chem.* **1992**, *96*, 7499.
(18) Gillie, J. K.; Small, G. J.; Golbeck, J. H. *J. Phys. Chem.* **1989**, *93*, 1620.
(19) Matthews, B. W.; Fenna, R. E. *Acc. Chem. Res.* **1980**, *13*, 309.
(20) Tronrud, D. E.; Schmid, M. F.; Matthews, B. W. *J. Mol. Biol.* **1986**, *188*, 443.
(21) Johnson, S. G.; Small, G. J. *Chem. Phys. Lett.* **1989**, *155*, 371.
(22) van Mourik, F.; Verwijst, R. R.; Mulder, J. M.; van Grondelle, R. *J. Lumin.* **1991**, *53*, 499.
(23) Lu, X.; Pearlstein, R. M. *Photochem. Photobiol.* **1993**, *57*, 86.
(24) Jankowiak, R.; Hayes, J. M.; Small, G. J. *Chem. Rev.* **1993**, *93*, 1471 and references therein.
(25) Johnson, S. G.; Lee, I.-J.; Small, G. J. In *Chlorophylls*; Scheer, H., Ed.; CRC Press: Boca Raton, FL, 1991; p 739.
(26) Kühlbrandt, W.; Wang, D. N. *Nature* **1991**, *350*, 130.
(27) Hemelrijk, P. W.; Kwa, S. L. S.; van Grondelle, R.; Dekker, J. P. *Biochim. Biophys. Acta* **1992**, *1098*, 159.
(28) Kwa, S. L. S.; Groeneveld, F. G.; Dekker, J. P.; van Grondelle, R.; van Amerongen, H.; Lin, S.; Struve, W. S. *Biochim. Biophys. Acta* **1992**, *1101*, 143.

(29) Krawczyk, S.; Krupa, Z.; Maksymiec, W. *Biochim. Biophys. Acta* **1993**, *1143*, 273.
(30) Kwa, S. L. S.; van Amerongen, H.; Lin, S.; Dekker, J. P.; van Grondelle, R.; Struve, W. S. *Biochim. Biophys. Acta* **1992**, *1102*, 202.
(31) Du, M.; Xie, X.; Mets, L.; Fleming, G. R. *Photochem. Photobiol.* **1993**, *57S*, 17S.
(32) Reddy, N. R. S.; Kolaczkowski, S. V.; Small, G. J. *J. Phys. Chem.* **1993**, *97*, 6934.
(33) Reddy, N. R. S.; Cogdell, R. J.; Zhao, L.; Small, G. J. *Photochem. Photobiol.* **1993**, *57*, 35.
(34) Shu, L.; Small, G. J. *Chem. Phys.* **1990**, *141*, 447.
(35) Shu, L.; Small, G. J. *J. Opt. Soc. Am. A* **1992**, *9*, 724.
(36) Friedrich, J.; Fischer, R.; Scheer, H. *J. Chem. Phys.* **1988**, *89*, 871.
(37) Due to interference from the antihole (on the high-energy side), hole width is better estimated as twice the lower-energy half-width at half-maximum intensity.
(38) Reddy, N. R. S.; Picorel, R.; Small, G. J. *J. Phys. Chem.* **1992**, *96*, 6458.
(39) Reddy, N. R. S.; Small, G. J.; Seibert, M.; Picorel, R. *Chem. Phys. Lett.* **1991**, *181*, 391.
(40) Hayes, J. M.; Gillie, J. K.; Tang, D.; Small, G. J. *Biochim. Biophys. Acta* **1988**, *932*, 287.
(41) Lee, I.-J.; Hayes, J. M.; Small, G. J. *J. Chem. Phys.* **1989**, *819*, 3463.
(42) van Mouik, F.; Visschers, R. W.; van Grondelle, R. *Chem. Phys. Lett.* **1992**, *193*, 1.
(43) Tang, D.; Jankowiak, R.; Small, G. J.; Tiede, D. M. *Chem. Phys.* **1989**, *131*, 99.
(44) Johnson, S. G.; Tang, D.; Jankowiak, R.; Hayes, J. M.; Small, G. J. *J. Phys. Chem.* **1990**, *94*, 5849.
(45) Warshel, W. A.; Parson, W. W. *J. Am. Chem. Soc.* **1987**, *109*, 6143.
(46) Losche, M.; Feher, G.; Okamura, M. Y. *Proc. Natl. Acad. Sci. U.S.A.* **1987**, *84*, 7537.
(47) Gillie, J. K.; Lyle, P. A.; Small, G. J. *Photosynth. Res.* **1989**, *22*, 233.
(48) Chang, H. C.; Jankowiak, R.; Picorel, R.; Seibert, M.; Yocum, C.; Small, G. J. *J. Phys. Chem.*, submitted.
(49) Ruban, A. V.; Horton, P. *Biochim. Biophys. Acta* **1992**, *1102*, 30.
(50) Jennings, R. C.; Bassi, R.; Garlaschi, F. M.; Dianese, P.; Zucchelli, G. *Biochemistry* **1993**, *32*, 3203.
(51) Zucchelli, G.; Dianese, P.; Jennings, R. C.; Breton, J.; Garlaschi, F. M.; Bassi, R. *Biochemistry*, submitted.
(52) Jennings, R. C.; Garlaschi, F. M.; Bassi, R.; Zucchelli, G.; Vianelli, A.; Dainese, P. *Biochim. Biophys. Acta* **1993**, *1183*, 194.
(53) Reddy, N. R. S.; Kolaczkowski, S. V.; Small, G. J. *Science* **1993**, *260*, 68.
(54) Kenney, M. J.; Jankowiak, R.; Small, G. J. *Chem. Phys.* **1990**, *146*, 47.
(55) Du, M.; Xie, X.; Mets, L.; Fleming, G. R. *J. Phys. Chem.*, following paper in this issue.
(56) Savikhin, S.; Zhou, W.; Blankenship, R. E.; Struve, W. S. *Biophys. J.* **1994**, *66*, 110.